2024 IEEE Transportation Electrification Conference and Expo (ITEC) | 979-8-3503-1766-4/24/$31.00 ©2024 IEEE | DOI: 10.1109/ITEC60657.2024.10599034

Reliable Fault-tolerant Distributed Control for Traction IPMSM in Electric Vehicle/Hybrid Electric Vehicle

Laxman Timilsina[1*], Payam R. Badr[2], Ali Arsalan [1], Gokhan Ozkan[1,3], Behnaz Papari[1,4], Christopher S. Edrington[1]
E-mails: {ltimils*, prameza, aarsala, gokhano, bpapari, cedring}@clemson.edu
[1]*Holcombe Department of Electrical and Computer Engineering, Clemson University, Clemson 29634, SC, USA*
[2]*Nexteer Automotive, Auburn Hills, 48326, MI, USA*
[3]*Dominion Energy Innovation Center, Clemson University, North Charleston 29405, SC, USA*
[4]*Department of Automotive Engineering, Clemson University, Greenville 29607, SC, USA*

***Abstract*—Electrical motors are used to provide traction power in electric/hybrid electric vehicles (EV/HEV). This paper introduces the concept of a distributed framework in which the task of traction drive control is shared between the local controllers. So, if one of the controllers is lost due to unforeseen circumstances such as faults, the neighboring agents can still drive the affected traction motor(s). Inverted-fed interior permanent magnet synchronous motors (IPMSM) are widely used for EV/HEV traction and are considered in a notional two-agent traction system case study. Each IPMSM controller includes a PI speed loop, a maximum torque per-ampere (MTPA) current reference generator, and space vector modulation (SVM) for inverter gate drive. The distributed framework generates global feedback variables between the neighboring agents to generate consensus input/output variables. Simulation results in the case study show promising reliability advantages in applying the proposed traction drive control framework.**

***Index Terms*—Traction motors, fault-tolerant distributed control, electric vehicles, interior permanent magnet synchronous motors**

I. Introduction

THE traction system configuration is one of the main differences between traditional internal combustion engine (ICE) and electric/hybrid-electric vehicles (EV/HEV). In ICE vehicles, the necessary torque for traction is generated in the engine and transmitted mechanically via mechanical components. EV/HEVs use electric machines, known as traction motors, with minimal mechanical components [1]. The latter configuration is more efficient than the former; however, traction motors require new electronic equipment for automated control through power electronic converters [2], [3]. The increased penetration of electronic equipment causes reliability concerns because of their susceptibility to faults and maintenance concerns [4], [5]. Consequentially, there is a higher risk that functionality losses in the electronic domain of the system translate into physical problems such as loss of traction. Thus, improving the reliability, resiliency, and robustness of the electronic equipment in EV/HEV is an important ongoing research and development problem.

There have been numerous studies on sensorless control methods that increase reliability by reducing dependency on physical measurements [6]–[9]. In general, these works propose some type of state observer and parameter estimation methods to reduce the control system's vulnerabilities to potential faults. For example, [9] use adaptive Kalman filters to formulate a sensor-fault-tolerant control for interior permanent magnet synchronous motors (IPMSM). Some recent research focus on the cyberattack detection and protection methods to reduce traction system vulnerabilities in EV/HEV [10]–[12].

Another way to approach the reliability problem is through distributed decision-making to avoid having a single point-offailure. Distributed control of dynamical systems using consensus protocols is a recognized topic in various applications, including power/energy management and converter control [13]–[15]. In [15], the authors show a distributed pulse width modulation for parallel inverters that feed an induction motor. The phase angle of the sinusoidal reference for each inverter is shared among the inverters; then, the current sharing is regulated by introducing the circulating current to adjust the sinusoidal references. The authors in [16] study the distributed control problem from the sensor network perspective, where a mixed model for the design, analysis, and synthesis of control algorithms within sensor networks is presented.

A. Statement Of Contributions

This paper studies the improvement of EV/HEV traction reliability by developing a distributed control framework via consensus protocols within the system. The control framework is designed such that if one "agent" is lost due to a fault, its associated motor does not lose its traction functionality. This

This work was supported by Clemson University's Virtual Prototyping of Autonomy Enabled Ground Systems (VIPR-GS) under Cooperative Agreement W56HZV-21-2-0001 with the US Army DEVCOM Ground Vehicle Systems Center (GVSC).

DISTRIBUTION STATEMENT A. Approved for public release; distribution is unlimited. (OPSEC 8129) is because the agents are interconnected to share information and duties; thus, there is no single point-of-failure [17]. Agents are defined here as the electronic equipment associated with each traction motor, i.e., controllers, measurement instruments, and communication links. The distributed traction benefits are verified in concept through simulation of a notional HEV's traction system with two IPMSM.

The rest of the paper is organized as follows. Section II presents the distributed consensus protocol and explains the control method's structure. Section III discusses the specifics of the example IPMSMs and the notional HEV and shows the test conditions and simulation results along with a discussion of notable takeaways. Finally, a summary of this paper's findings and potential future works are given in Section IV.

II. DISTRIBUTED TRACTION CONTROL

A. Control paradigm

The diagram in Fig. 1 shows how these different parts of the distributed control are interconnected with one another for a notional two-agent IPMSM traction system. Note that the proposed distributed framework is applicable in theory to different traction configurations with an arbitrary number of agents. In the following subsections, different components of the distributed control paradigm will be individually introduced.

B. Consensus variables

Each controller executes its decision-making based on three external information, which are winding currents (i_{ab}), and rotor speed (ω_m) gathered from local and neighboring agents. Thus, a consensus must be reached regarding these variables to achieve distributed control. The interaction between agents is defined using graph theory. Let the communication network be represented by a directed graph $\mathcal{G} := (\nu, \epsilon)$, where $\nu \in \mathbb{R}^N$ is the set of nodes associated with N neighboring agents in the system, and E is the set of communication links between the agents. In this study, it is assumed there are two communication links per agent in the neighborhood; that is, one for input and one for output.

A binary matrix that indicates the operational status of each agent is defined as $\mathcal{S} \in \mathbb{R}^{NN}$ where its diagonal indices (s_{ii}) are 1 if controller i is online. The off-diagonal indices ($s_{ij}, i \neq j$) are set if communication from agent j to i is online. Considering the previous definitions, the global consensus variables are calculated as follows.

$$\hat{x}_i = \frac{1}{\sum_{j=1}^{N} g_{ij} sij} \sum_{j=1}^{N} g_{ij} s_{ij} x_j \tag{1}$$

Where x_j is variable data received from agent j, and $\hat{x}_i$ is the consensus variable in agent i. $\mathcal{G} = [g_{ij}] \in \mathbb{R}^{NXN}$ is a gain matrix with its diagonal indices weighting local information and its off-diagonal indices weight neighboring information.

C. Local control method

Each controller has two tasks: speed control and inverter gate modulation. The speed control mechanic is consisted of a PI controller and maximum torque-per-ampere (MTPA) reference generator [18]. The inverter modulation generates the appropriate switching signals based on reference set points from the speed controller. There are a variety of inverter modulation methods available, among which space vector modulation (SVM) is widely used. Thus, SVM is also used for the purposes of this study [19], [20].

1) Speed control: The speed controller generates an appropriate torque reference (τ^*) considering the speed error at each time step. The PI speed controller function is as follows.

$$\tau^* = K_P.e_\omega(t) + K_I.\int_{t_0}^{t_1} e_\omega(t)dt \tag{2a}$$

$$e_\omega(t) = \omega_m^* - \hat{\omega}_m(t) \tag{2b}$$

Where K_P and K_I are the proportional and integral gains, respectively. ω_m^* is the reference angular speed command requested by the driver or autonomous driving program.

IPMSM has PMs embedded into the rotor structure, which generate magnetic saliency. This magnetic saliency produces a reluctance torque because of the resulting difference between the d-axis (L_d) and q-axis (L_q) inductances. Maximum efficiency can be achieved in IPMSM by properly selecting a current vector ratio between magnetic torque current (i_q^*) and reluctance torque current (i_d^*) satisfying the total current magnitude (I_m) constraint [21]. There are two modes of operation in IPMSM: 1) constant torque, 2) constant power (field-weakening), which are determined based on rotor speed. If $\hat{\omega}_m$ is less than the base speed ($\hat{\omega}_m \leq \omega_b$), the IPMSM is in the constant torque mode, and if $\hat{\omega}_m > \omega_b$, it is in constant power mode. Calculating the appropriate (i_q^*, i_d^*) to achieve MTPA in constant torque and power regions is shown in (3a).

$$I_m = \sqrt{{i_d^*}^2 + {i_q^*}^2} = \frac{2}{3p\lambda_f}\tau^* \tag{3a}$$

$$i_d^* = \begin{cases} \frac{\lambda_f}{4(L_q - L_d)} - \sqrt{\frac{{\lambda_f}^2}{16(L_q - L_d)^2} + \frac{I_m^2}{2}} & \omega_m \leq \omega_b \\ \frac{-\lambda_f L_d + \sqrt{(\lambda_f)^2 - (L_q^2 - L_d^2)(\lambda_f^2 + L_q^2 I_m^2 - \frac{v_{max}^2)}{\omega_e^2}}}{(L_q^2 - L_d^2)} & \omega_m > \omega_b \end{cases} \tag{3b}$$

$$i_q^* = \sqrt{I_m^2 - {i_d^*}^2} \tag{3c}$$

Where p is the number of pole pairs, and λ_f is the PM flux linkage. v_{max} is the maximum peak fundamental line to the neutral voltage supplied to the motor and is calculated as follows.

$$v_{d0} = -\omega_e L_q i_q \tag{4a}$$

$$v_{q0} = -\omega_e(L_d i_d + \lambda_f) \tag{4b}$$

$$v_{max} = \sqrt{v_{do}^2 + v_{qo}^2} \tag{4c}$$

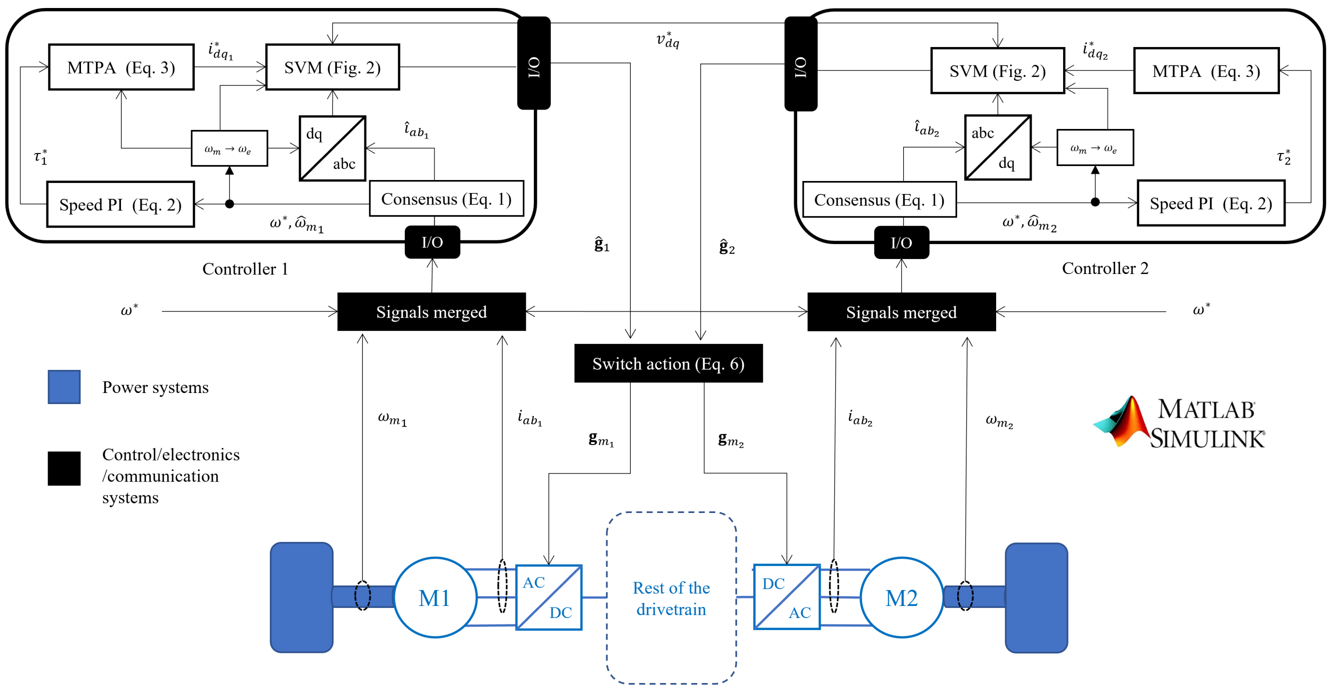

Fig. 1. The overall schematic of the distributed traction system.

Where v_{d0} and v_{q0} are the d-axis voltage when i_d is zero, and the q-axis voltage when i_q is zero, respectively. $\omega_e = p\omega_m$ is the electrical angular rotor speed.

2) Space vector modulation: The inverter type is assumed to be three-phase neutral-point-clamped (NPC) which are proven to offer better overall performance in traction motors [22]. There are 27 voltage vectors (19 independent) available in three-level converters. The SVM strategy is based on selecting the appropriate voltage vector sectors and subsectors, then calculating their gating times. Interested readers are encouraged to read [23] for more information about the SVM in three-level converters. The overall flowchart of the SVM strategy is shown in Fig. 2.

D. Output consensus

The consensus gate signals generated by each controller ($\hat{g}_i$) are passed through a signal switching mechanic before reaching the inverter gate drivers. The purpose of this gate signal processing, which is described in (5), is to improve reliability in situations where an agent's output is lost. It must be emphasized that only physical faults that cause an agent's controller or I/O communication to be fully or partially lost are studied in this paper.

$$g_{m_i} = \begin{cases} \hat{g}_i & s_{ii} = 1 \\ \hat{g}_j & s_{ii} = 0 \ \& \ s_{ij} = 1 \ \& \ s_{ji} = 1 \end{cases} \tag{5}$$

Where g_{m_i} is the final gate signal sent to the $i-th$ motor in the distributed neighborhood.

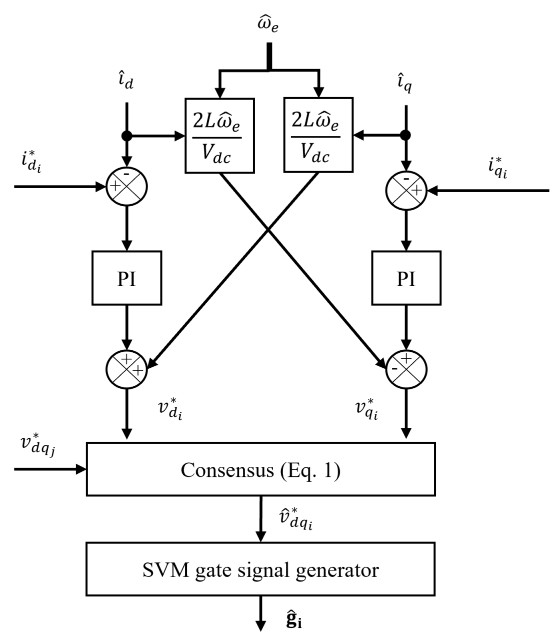

Fig. 2. SVM gate signal generation flowchart.

III. CASE STUDY

A. Example Motor and Vehicle

The two IPMSMs used in the example traction system are identical 120 kW eight-pole machines with some of the relevant parameters shown in Table I [24]. The IPMSMs are modeled using a fourth-order state-space equation as described in (6) [25].

$$\begin{bmatrix} \dot{i}_d \\ \dot{i}_q \\ \dot{\omega}_m \\ \dot{\theta}_m \end{bmatrix} = \begin{bmatrix} -\frac{R_s}{L_d} & \frac{L_q}{L_d}p\omega_m & 0 & 0 \\ -\frac{L_d}{L_q}p\omega_m & -\frac{R_s}{L_q} & -\frac{\lambda_f}{L_q}p & 0 \\ \frac{3}{2J_{eq}}p(L_d - L_q)i_q & \frac{3}{2J_{eq}}p\lambda_f & -\frac{1}{J_{eq}}\eta & 0 \\ 0 & 0 & 1 & 0 \end{bmatrix} \begin{bmatrix} i_d \\ i_q \\ \omega_m \\ \theta_m \end{bmatrix} + \begin{bmatrix} \frac{1}{L_d} & 0 & 0 \\ 0 & \frac{1}{L_q} & 0 \\ 0 & 0 & -\frac{1}{J_{eq}} \\ 0 & 0 & 0 \end{bmatrix} \begin{bmatrix} v_d \\ v_q \\ \tau_m \end{bmatrix} \tag{6}$$

Where R_s is the average winding resistance per phase. η is the rotor damping coefficient. $\omega_m, \theta_m, J_{eq}$, and τ_m are the mechanical angular speed, rotor angular position, the equivalent inertia as seen by the motor shaft, and the terrain load torque, respectively. J_{eq} is approximately estimated using the vehicle's properties [26].

TABLE I
EXAMPLE IPMSM TRACTION SYSTEM SPECIFICATIONS

Base speed	6500 rpm
Max. speed	10,000 rpm
Pole pairs	4
Max. winding current mag.	480 A
Winding resistance	0.01267 Ω
dq-axis inductances	0.1901, 0.4528 mH
PM flux linkage	0.07 V.s
Vehicle mass	5,000 lbs
Gear ratio	7.938
Rolling resistance coefficient	0.045
Wheel radius	15 in

B. Simulation

Simulations are conducted with with MATLAB/Simulink for three fault scenarios which are modeled by changing the status matrix $\mathcal{S} \in \mathbb{R}^{NxN}$. The fault scenarios are as follows.

1) The controller in agent 2 is out ($s_{22} = 0$).
2) The communication from agent 2 to agent 1 is lost ($s_{12} = 0$).
3) Agent 2 (communication and controller) is entirely offline ($s_{22} = 0$ and $s_{12} = 0$).

The faults are introduced at $t = 1\ s$. The load torque in test scenarios for IPMSM 1 is $\tau_{m_1} = 10N.m$ and $\tau_{m_2} = 20N.m$. The load torques are chosen differently to reflect circumstances where the terrain conditions are not symmetrical about one axle of the vehicle. However, in rare occasions that one side of the axel experiences loads several orders of magnitude different from the other side, a separate torque distribution control would be necessary to adaptively adjust distributed control gains, i.e., $\mathcal{G} = [g_{ij}] \in \mathbb{R}^{NxN}$, which is constant in this case study. The same problem exists if the rear and front traction systems were to be integrated as distributed neighbors since front and rear load conditions are not similar.

The speed tracking and the electromagnetic torque output of the IPMSMs in the traction system for all three faulted operation scenarios are shown in Fig. 3. It is evident that both IPMSM motors remain operational by generating electromagnetic torque to support vehicle traction. The speed tracking steady-state error in IPMSM 1 is 6.52 rpm at its worst and 10.36 rpm in IPMSM 2, which occurs in scenario 2 (communication loss). The electromagnetic torque output of IPMSM 2 has its highest fluctuation in scenario 3 at 138 $N.m$ in 20 ms. The oscillations in the torque outputs damp as the motors reach steady-state, but sustained oscillations are more conspicuous in IPMSM 2, as shown in Fig. 6.

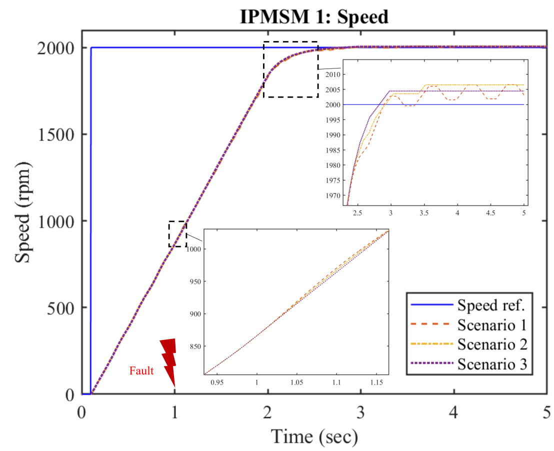

Fig. 3. The speed tracking performance output of IPMSM 1 in each fault scenario.

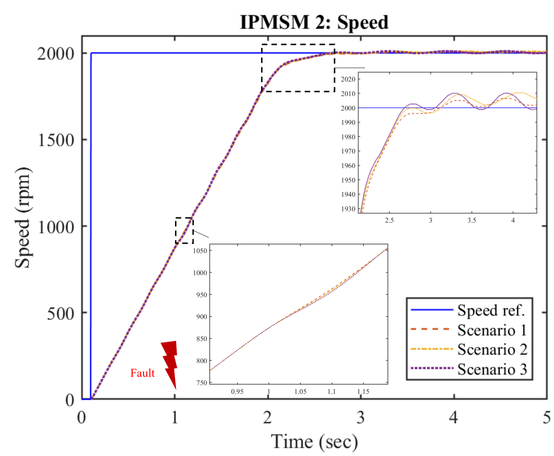

Fig. 4. The speed tracking performance output of IPMSM 2 in each fault scenario.

IV. Conclusion

This paper presented a framework for distributed traction control in EV/HEV applications to improve reliability. The distributed traction control was tested for a notional HEV traction system with two IPMSMs. The simulation results

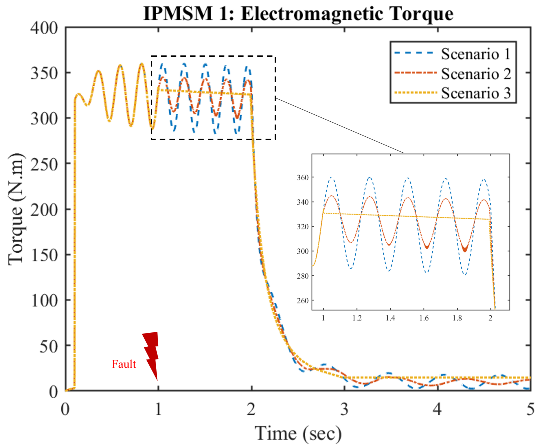

Fig. 5. The electromagnetic torque output of IPMSM 1 in each fault scenario.

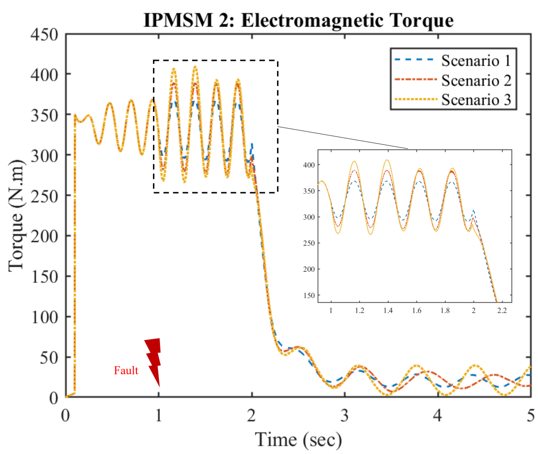

Fig. 6. The electromagnetic torque output of IPMSM 2 in each fault scenario.

indicated that it is possible, in concept to improve traction reliability by integrating the control decision-making processes. Because there is no single point-of-failure in the system, if one agent partially or fully loses its functionality, the other agent compensates for this failure and drives both motors based on the available information. Some potential future research prospects are: 1) integrated controller-hardware-in-the-loop experiments for real-time tests using standard automotive drive cycles, 2) expanding the number of motors in the distributed traction neighborhood, 3) considering all-wheel drivetrains, which require optimal torque sharing, and 4) study of cyberattack-induced faults in the traction system and the means to detect and mitigate their impact.

Acknowledgment

This work was supported by Clemson University's Virtual Prototyping of Autonomy Enabled Ground Systems (VIPR-GS) under Cooperative Agreement W56HZV-21-2-0001 with the US Army DEVCOM Ground Vehicle Systems Center (GVSC).

DISTRIBUTION STATEMENT A. Approved for public release; distribution is unlimited. (OPSEC 8129)

The authors would like to acknowledge the Warren H. Owen Distinguished Professorship Endowment for its support of the research effort.

References

[1] K. C¸ . Bayindir, M. A. G¨oz¨uk¨uc¸ ¨uk, and A. Teke, "A comprehensive overview of hybrid electric vehicle: Powertrain configurations, powertrain control techniques and electronic control units," *Energy conversion and Management*, vol. 52, no. 2, pp. 1305–1313, 2011.

[2] S. J. Rind, Y. Ren, Y. Hu, J. Wang, and L. Jiang, "Configurations and control of traction motors for electric vehicles: A review," *Chinese Journal of Electrical Engineering*, vol. 3, no. 3, pp. 1–17, 2017.

[3] A. Emadi, Y. J. Lee, and K. Rajashekara, "Power electronics and motor drives in electric, hybrid electric, and plug-in hybrid electric vehicles," *IEEE Transactions on Industrial Electronics*, vol. 55, no. 6, pp. 2237–2245, 2008.

[4] L. Timilsina, P. H. Hoang, A. Moghassemi, E. Buraimoh, P. K. Chamarthi, G. Ozkan, B. Papari and C. S. Edrington, "A Real-time Prognostic-based Control Framework for Hybrid Electric Vehicles," *IEEE Access*, vol. 11, pp. 42431-42462, 2023.

[5] L. Timilsina, P. H. Hoang, A. Arsalan, G. Ozkan, B. Papari, and C. S. Edrington, "Degradation Abatement In Hybrid Electric Vehicles Using Data-driven Technique", *Transportation Research Procedia*, 2023.

[6] Z. Chen, M. Tomita, S. Doki, and S. Okuma, "An extended electromotive force model for sensorless control of interior permanent-magnet synchronous motors," *IEEE transactions on Industrial Electronics*, vol. 50, no. 2, pp. 288–295, 2003., Philadelphia, PA, USA, 2006, pp. 1-7.

[7] S. Ling, T. Shi, Z. Lin, Q. Geng, and C. Xia, "Interior permanent magnet synchronous motor maximum torque per ampere-position sensorless control," *IEEE Applied Power Electronics Conference and Exposition (APEC)*, IEEE, 2019, pp. 2589–2596.

[8] M. F. Rahman, L. Zhong, M. E. Haque, and M. Rahman, "A direct torque-controlled interior permanent-magnet synchronous motor drive without a speed sensor," *IEEE Transactions on Energy Conversion*, vol. 18, no. 1, pp. 17–22, 2003.

[9] F. Mwasilu and J.-W. Jung, "Enhanced fault-tolerant control of interior pmsms based on an adaptive ekf for ev traction applications," *IEEE Transactions on Power Electronics*, vol. 31, no. 8, pp. 5746–5758, 2015.

[10] L. Timilsina, P. R. Badr, P. H. Hoang, G. Ozkan, B. Papari and C. S. Edrington, "Battery Degradation in Electric and Hybrid Electric Vehicles: A Survey Study," *IEEE Access*, vol. 11, pp. 42431-42462, 2023.

[11] B. Yang, J. Ye, and L. Guo, "Fast detection for cyber threats in electric vehicle traction motor drives," *IEEE Transactions on Transportation Electrification*, vol. 8, no. 1, pp. 767–777, 2021.

[12] L. Guo and J. Ye, "Cyber-physical security of electric vehicles with four motor drives," *IEEE Transactions on Power Electronics*, vol. 36, no. 4, pp. 4463–4477, 2021.

[13] L. Timilsina, A. Moghassemi, E. Buraimoh, A. Arsalan, P.K. Chamarthi, G. Ozkan, B. Papari and C. S. Edrington, "Impact of Vehicle-to-Grid (V2G) on Battery Degradation in a Plug-in Hybrid Electric Vehicle," *SAE Technical Paper*, 2024.

[14] X. Chen, M. Shi, J. Zhou, Y. Chen, W. Zuo, J. Wen, and H. He, "Distributed cooperative control of multiple hybrid energy storage systems in a dc microgrid using consensus protocol," *IEEE Transactions on Industrial Electronics*, vol. 67, no. 3, pp. 1968–1979, 2019.

[15] M. Hua, H. Hu, Y. Xing, and Z. He, "Distributed control for ac motor drive inverters in parallel operation," *IEEE Transactions on Industrial Electronics*, vol. 58, no. 12, pp. 5361–5370, 2011.

[16] B. Sinopoli, C. Sharp, L. Schenato, S. Schaffert, and S. Sastry, "Distributed control applications within sensor networks," *Proceedings of the IEEE*, vol. 91, no. 8, pp. 1235–1246, 2003.

[17] E. Gumrukcu, A. Arsalan, G. Muriithi, C. Joglekar, A. Aboulebdeh, M. Alparslan Zehir, B. Papari, and A. Monti, "Impact of cyber-attacks on ev charging coordination: The case of single point of failure," *4th Global Power, Energy and Communication Conference (GPECOM)*, 2022, pp. 506–511.

[18] S. Morimoto, M. Sanada, and Y. Takeda, "Wide-speed operation of interior permanent magnet synchronous motors with high-performance current regulator," *IEEE Transactions on Industry Applications*, vol. 30, no. 4, pp. 920–926, 1994.

[19] Y. Wang, X. Wang, W. Xie, F. Wang, M. Dou, R. M. Kennel, R. D. Lorenz, and D. Gerling, "Deadbeat model-predictive torque control with discrete space-vector modulation for pmsm drives," *IEEE Transactions on Industrial Electronics*, vol. 64, no. 5, pp. 3537–3547, 2017.

[20] V. Jayakumar, B. Chokkalingam, and J. L. Munda, "A comprehensive review on space vector modulation techniques for neutral point clamped multi-level inverters," *IEEE Access*, vol. 9, pp. 112 104–112 144, 2021.

[21] S. Lim, "Sensorless-foc with flux-weakening and mtpa for ipmsm motor drives," Texas Instruments, Tech. Rep., 2018. .

[22] A. Poorfakhraei, M. Narimani, and A. Emadi, "A review of multilevel inverter topologies in electric vehicles: Current status and future trends," *IEEE Open Journal of Power Electronics*, vol. 2, pp. 155–170, 2021 .

[23] J. H. Seo, C. H. Choi, and D. S. Hyun, "A new simplified space-vector pwm method for three-level inverters," *IEEE Transactions on power electronics*, vol. 16, no. 4, pp. 545–550, 2001.

[24] P. R. Badr, G. Ozkan, P. Hoang, C. S. Edrington, and T. Parker, "Multi-objective finite control set model predictive control for interior permanent magnet motors in electric/hybrid-electric vehicles," *SAE Technical Paper*, Tech. Rep., 2022. .

[25] M. Boussak, "Implementation and experimental investigation of sensorless speed control with initial rotor position estimation for interior permanent magnet synchronous motor drive," *IEEE Transactions on Power Electronics*, vol. 20, no. 6, pp. 1413–1422, 2005.

[26] P. Fajri, R. Ahmadi, and M. Ferdowsi, "Equivalent vehicle rotational inertia used for electric vehicle test bench dynamic studies," *IECON 2012-38th Annual Conference on IEEE Industrial Electronics Society*, IEEE, 2012, pp. 4115–4120.